SPIN-POLARIZATION SIMULATIONS FOR THE FUTURE CIRCULAR COLLIDER E+E- USING BMAD[*]

Y. Wu[1][†], F. Carlier[2], D. P. Barber[3], L. van Riesen-Haupt[1], E. Gianfelice-Wendt[4], T. Pieloni[1]
[1]EPFL, Lausanne, Switzerland, [2]CERN, Geneva, Switzerland
[3]University of New Mexico, NM, USA, [4]Fermilab, IL, USA

Abstract

The high precision measurement of the centre-of-mass energy in the Future Circular Collider e+e- (FCC-ee) at Z and W energies can be realized through resonant spin depolarization utilizing transversely polarized beams. This requires a guaranteed sufficiently-high spin polarization in the presence of lattice imperfections. Investigations of the impact of misalignments on the equilibrium polarization are conducted using analytical and Monte-Carlo spin simulations with Bmad. Potential optimization schemes to ensure high polarization using orbit bumps have been explored.

INTRODUCTION

The Future Circular Collider (FCC) project aims to provide unprecedented opportunities for high-energy physics research by exploring the electroweak and Higgs sectors, top quark physics, and by searching for new physics beyond the Standard Model [1]. The FCC-ee is the electron-positron collider envisaged for the first phase of the FCC project [2]. The planned centre-of-mass energy of the FCC-ee ranges from 88 GeV to 365 GeV, to cover the energies from Z^0 bosons (91 GeV) to the $t\bar{t}$ threshold ($350 - 365$ GeV) [1].

The current targets for the precision of energy calibration at the Z and W energies are 4 keV and 100 keV respectively [3], and it is expected that they can be realized using resonant depolarization with radio-frequency external electromagnetic fields [4]. For this, at least 10% beam polarization should be maintained in the presence of various misalignments [4]. Thus calculations of spin polarization have been undertaken to investigate the influence of lattice imperfections on polarization [5–7]. In this investigation, the equilibrium polarization levels near the Z energy (45.6 GeV) are estimated using the software package Bmad [8] with its facilities for analytical linearized spin-orbit motion and for 3-D Monte-Carlo spin-orbit tracking simulations. Both are exploited here. In this report, we focus on the use of special closed-orbit bumps to alleviate the effects of misalignments. Two possible optimization schemes are employed, the HERA formalism [9, 10] and the Rossmanith-Schmidt scheme [11, 12], and their efficacies are compared.

The Basics of Electron (Positron) Spin Dynamics

Particle spins precess in electromagnetic fields according to the T-BMT equation [13, 14]

$$\frac{\mathrm{d}\vec{S}}{\mathrm{d}t} = \vec{\Omega}_{\mathrm{BMT}} \times \vec{S}, \tag{1}$$

where $\vec{S}$ is the single-particle spin-expectation value and $\vec{\Omega}_{\mathrm{BMT}}$ is the precession vector. The unit-length periodic solution on the closed orbit is denoted by $\hat{n}_0$. In a perfectly aligned flat ring without solenoids, $\hat{n}_0$ is vertical and the closed-orbit spin tune ν_0, i.e. the number of precessions per turn around $\hat{n}_0$ performed by spins on the closed orbit, is $a\gamma$, where a is the gyromagnetic anomaly and γ is the Lorentz factor, while ν_0 deviates from $a\gamma$ in the presence of lattice imperfections [16].

The spin polarization of stored electron (positron) beams builds up naturally by synchrotron radiation emission to a theoretical maximum level of 92.38% in uniform magnetic fields [17]. This is the Sokolov-Ternov (ST) effect [17]. Meanwhile, the spin diffusion due to stochastic photon emissions combined with non-uniform magnetic fields induces radiative depolarization [16] which exerts a counteracting influence. The beam polarization builds up along $\hat{n}_0$ and by the Derbenev-Kondratenko (DK) formula [18, 19] reaches

$$P_{dk} = \mp \frac{8}{5\sqrt{3}} \frac{\oint \mathrm{d}s \left\langle \frac{1}{|\rho(s)|^3} \hat{b} \cdot \left(\hat{n} - \frac{\partial \hat{n}}{\partial \delta} \right) \right\rangle_s}{\oint \mathrm{d}s \left\langle \frac{1}{|\rho(s)|^3} \left(1 - \frac{2}{9} (\hat{n} \cdot \hat{s})^2 + \frac{11}{18} \left(\frac{\partial \hat{n}}{\partial \delta} \right)^2 \right) \right\rangle_s}$$

for electrons (positrons) where ρ is the bending radius, $\hat{b} = (\hat{s} \times \dot{\hat{s}})/|\dot{\hat{s}}|$ is the direction of the magnetic field and $\hat{n}$ is the "*invariant spin field*" [15] which depends on phase space and azimuthal positions $(x, p_x, y, p_y, z, \delta; s)$. The term $(\partial \hat{n}/\partial \delta)^2$ accounts for the radiative depolarization. The beam polarization builds up from an initial value P_0 as [16]

$$P(t) = P_{dk} \left[1 - e^{-t/\tau_{dk}} \right] + P_0 e^{-t/\tau_{dk}} \tag{2}$$

for which the build-up rate τ_{dk} can be written as [16]

$$\frac{1}{\tau_{dk}} = \frac{1}{\tau_{bks}} + \frac{1}{\tau_{dep}}, \tag{3}$$

where τ_{bks} is the Baier-Katkov-Strahkovenko (BKS) build-up rate for arbitrary magnetic guide fields without including radiative depolarization, and τ_{dep} is the depolarization rate.

When the spin precession is coherent with the perturbations from synchro-betatron oscillations, i.e., when ν_0 and the synchro-betatron tunes $Q_{x,y,z}$ satisfy the resonance relation [1] [16]

$$\nu_0 = k + k_x Q_x + k_y Q_y + k_z Q_z, \tag{4}$$

---
[1] It suffices here to use ν_0 instead of the amplitude-dependent spin tune [20] in the expression for the resonance condition.

where k and $k_{x,y,z}$ are integers, strong depolarization can occur. The order of a resonance is $|k_x|+|k_y|+|k_z|$, with $|k_x|+|k_y|+|k_z|= 1$ for first order.

ENERGY SCANS WITH LINEARIZED AND 3-D SPIN MOTION

For our study, we use the FCC-ee V217 lattice at the Z pole [21]. Misalignments and angular deviations of all elements are modeled and generated from truncated Gaussian distributions [5, 7].

The equilibrium polarization calculated by Tao (Bmad) [22] at first order i.e., with linearized spin-orbit motion to obtain $(\partial\hat{n}/\partial\delta)^2$ in the DK formula [16], demonstrates the influence of first-order resonances, while tracking with 3-D spin motion and radiation exposes the higher-order resonances and plays a key role in evaluating the overall impact of lattice imperfections. The depolarization rate τ_{dep} from tracking can be extracted from the variation of the polarization starting from P_0, and fitting the evolution curve $P(t) \simeq P_0 e^{-t/\tau_{dep}}$. Next, with the DK formula for a nominally flat ring, one sees that the equilibrium polarization with τ_{dep} calculated at first order or got by tracking can be well approximated as

$$P_{eq} \simeq P_{bks} \frac{1}{1 + \tau_{bks}/\tau_{dep}}, \qquad (5)$$

where P_{bks} is the BKS polarisation level [16].

Figure 1 shows P_{eq} in energy scans with linearized and 3-D spin motion using the same error seed that induces 43.7 μm rms vertical orbit distortion. For the 3-D tracking simulations 1000 electrons are tracked for over 7000 turns using the Long-Term Tracking module [23]. The first-order spin-orbit resonances are recognizable, while the higher order resonances, such as the two synchrotron sidebands of one of the parent vertical resonance $\nu_0 = k + Q_y$, can be observed in the 3-D spin trackings. The sensitivity of polarization to the orbit distortion justifies the demands for a high-standard orbit correction and optics tuning.
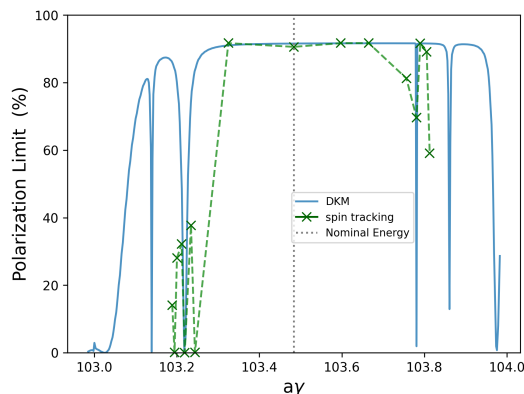

Figure 1: Polarization levels from first-order analytical τ_{dep} and Monte-Carlo tracking using V217 lattice [5]

HARMONIC SPIN MATCHING SCHEMES

In the presence of misalignments, $\hat{n}_0$ is not vertical everywhere but experiences a deviation $\delta\hat{n}_0$, which together with the horizontal orbital oscillations, tends to lead to the strongest source of spin diffusion [9]. However, $\delta\hat{n}_0$ can be reduced and the polarization increased by using multiple vertical orbit correctors to create a controllable $\hat{n}_0$ tilt and reduce $(\delta\hat{n}_0)_{rms}$ [9]. Thus closed vertical bumps, each consisting of three vertical orbit correctors in arc sections, are used to generate additional tilt for correction without influencing the closed orbit overall. The HERA formalism [9,10] and Rossmanith-Schmidt scheme [11, 12] are two promising spin matching schemes that can be used in the FCC-ee and we study them using the FCC-ee V22 lattice [24] together with an effective lattice with 72 μm rms vertical orbit distortion to simulate the ring after correction.

Simplified HERA Formalism

In the HERA formalism, the $\delta\hat{n}_0$ can be written as [9]

$$\delta\hat{n}_0 = \alpha\hat{m} + \beta\hat{l}, \qquad (6)$$

where $\hat{m}$, $\hat{l}$ and $\hat{n}_0$ comprise a 1-turn-periodic orthonormal basis on the design orbit. Under Fourier analysis of the perturbations causing closed-orbit distortion, and then the tilt $\delta\hat{n}_0$, we have

$$(\alpha - i\beta)(s) = -i\frac{C}{2\pi} \sum_k \frac{f_k}{k - \tilde{\nu}} e^{i2\pi ks/C}, \qquad (7)$$

where C is the circumference, k is an integer, $\tilde{\nu}$ is the fractional part of the spin tune, and the f_k are the Fourier coefficients related to the perturbations [9]. Then the harmonics for $k = 0$ and $k = 1$, making the largest contribution, should be minimized.

The simplified HERA formalism used here takes simulated information on the direction of $\hat{n}_0$ at every element, expands $n_{0x}(s) + in_{0z}(s)$ into a Fourier series and minimizes Fourier coefficients of harmonics 0 and 1 using four closed vertical bumps. The strength of the first corrector is the independent variable of a closed bump, and each bump has a linear contribution to the harmonics, which is expressed as $\mathbf{MK} = \mathbf{C}$, where $\mathbf{K}$ is the column matrix of bump amplitudes, and $\mathbf{C}$ contains the real and imaginary parts of the Fourier coefficients of harmonics 0 and 1. In order to correct $\delta\hat{n}_0$ in a misaligned ring with the coefficients for harmonics 0 and 1 being $\mathbf{A}$, the required bump amplitudes are estimated via $\mathbf{K} = \mathbf{M}^{-1}(-\mathbf{A})$. The matrix $\mathbf{M}$ is obtained by analyzing the contribution to the vector of a single closed bump in every possible location in a lattice without errors and selecting stored vectors of four locations out of them. The best bump locations correspond to the ones that create the largest determinant of $\mathbf{M}$, so that the same correction effect is achieved with the smallest orbit distortion [9].

The correction is conducted at 45.82 GeV ($a\gamma = 103.983$) which is close to the integer resonance $\nu_0 = 104$ and where $\hat{n}_0$ experiences larger deviation. Figure 2 shows the polarization curves for first-order τ_{dep} near the Z energy with

and without the correction scheme. By using four bumps optimized at $a\gamma = 103.983$, $(\delta\hat{n}_0)_{\mathrm{rms}}$ is decreased from 2.28 mrad to 0.90 mrad and the polarization is elevated from 10.68% to 90.96% by the suppression of the nearby first-order parent synchrotron resonance. Although the polarization near 104 is largely improved when bumps are set at 45.82 GeV, the level near 103 is reduced while the level far from integer resonances is unaffected. Thus the simplified HERA formalism is shown to be locally effective for $\delta\hat{n}_0$ correction and polarization improvement.
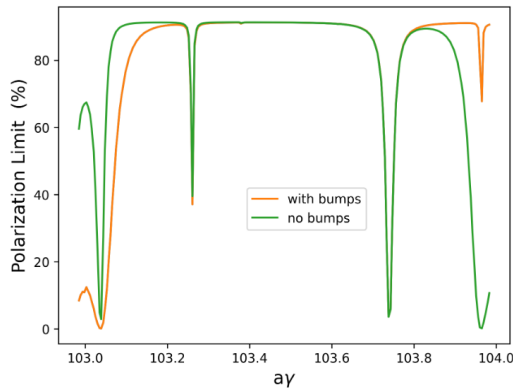

Figure 2: Polarization levels from first-order analytical τ_{dep} with and without harmonic bumps optimized at 45.82 GeV ($a\gamma = 103.983$) using the HERA formalism in V22 lattice

The complete HERA formalism is a rigorous and systematic approach that relies on the analysis of $\delta\hat{n}_0$. This is too small to be directly accessible with a polarimeter. So empirical bump adjustments based on the feedback from polarization measurements are inevitable. These can be made practical by using wigglers which are to be used to lessen the polarization build-up time of pilot bunches used for energy calibration. Ways to apply the complete HERA formalism in spin simulation are under investigation.

Rossmanith-Schmidt Scheme

By assuming that the spin precession around vertical direction takes place only in bending magnets, and the radial perturbing fields on the closed orbit only exist between bending magnets, the Rossmanith-Schmidt scheme formulates $\delta\hat{n}_0$ as [11],

$$|\delta\vec{n}_0| = \frac{(1 + a\gamma)}{2(1 - \cos 2\pi a\gamma)} \left[\left(\sum_{i=1}^{N} \sin(a\gamma\theta_i)\Delta y_i' \right)^2 + \left(\sum_{i=1}^{N} \cos(a\gamma\theta_i)\Delta y_i' \right)^2 \right],$$

(8)

where θ_i is the accumulated deflecting angle after ith bending magnet, and $\Delta y_i'$ is the change of vertical closed orbit angle between two adjacent dipoles. The function $\Delta y'(\theta)$ can be expanded into a Fourier series [11, 12]

$$\Delta y'(\theta) = \sum_{k=1}^{\infty} (a_k \cos k\theta + b_k \sin k\theta),$$

(9)

where

$$\begin{aligned} a_k \\ b_k \end{aligned} = \frac{1}{N} \sum \Delta y_i'(\theta_i) \begin{aligned} \cos k\theta_i \\ \sin k\theta_i \end{aligned}.$$

(10)

The ks which are adjacent to $a\gamma$ make the biggest contributions to the sum. For this demonstration, Fourier coefficients of $k = 103$ and $k = 104$ are minimized using four closed bumps optimized at 45.82 GeV. Figure 3 shows the polarization curves for first-order τ_{del} before and after applying bumps set at 45.82 GeV. The $(\delta\hat{n}_0)_{\mathrm{rms}}$ is decreased from 2.28 mrad to 0.90 mrad at 45.82 GeV, with the polarization being elevated from 10.68% to 89.65% with the weakening of the first-order parent synchrotron resonance. The first-order synchrotron resonance near $k = 103$ is also weakened so that the polarization near both 103 and 104 is improved using this scheme. This weakening of the first-order resonances would also weaken the highly-depolarizing synchrotron sidebands.
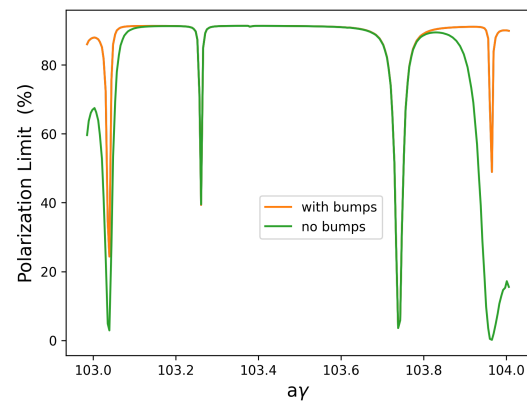

Figure 3: Polarization levels from first-order analytical τ_{dep} with and without harmonic bumps optimized at 45.82 GeV ($a\gamma = 103.983$) using the Rossmanith-Schmidt scheme in V22 lattice

The Rossmanith-Schmidt scheme is less general than the HERA formalism. Applying it directly in a real ring requires the knowledge of y' of the closed orbit at every dipole. This could be solved by mounting BPMs at both ends of each dipole. However, the additional high cost it brings and the influence of BPM misalignments and calibration errors are the main obstacles to applying this scheme.

CONCLUSIONS AND OUTLOOK

Spin simulations are pivotal for revealing the impact of lattice imperfections on the attainable level of polarization. Both first-order analytical and Monte-Carlo spin simulations have been performed for the FCC-ee using Bmad, and the equilibrium polarization near the nominal energy remains high in the effective lattice employed. After a conventional lattice correction, two spin matching schemes, the HERA formalism and the Rossmanith-Schmidt scheme, are effective for correcting $\delta\hat{n}_0$ and for improving the polarization level. The challenges around applying these schemes in the real ring are under investigation. The spin matching strategy that relies on the analysis of the beam-based observables is the focus of the ongoing research.

REFERENCES

[1] A. Abada *et at.*, "FCC Physics Opportunities: Future Circular Collider Conceptual Design Report Volume 1", *Eur. Phys. J. C*, vol. 79, p. 474, 2019.
doi:10.1140/epjc/s10052-019-6904-3

[2] A. Abada *et at.*, "FCC-ee: The Lepton Collider: Future Circular Collider Conceptual Design Report Volume 2", *Eur. Phys. J. Spec. Top.*, vol. 228, pp. 261–623, 2019.
doi:10.1140/epjst/e2019-900045-4

[3] A. Blondel, "PED Overview: Centre-of-mass energy calibration", Accessed 24/04/2023,
https://indico.cern.ch/event/1064327/contributions/4893236/attachments/2452727/4203106/EPOL\%202022-05-30.pdf

[4] A. Blondel *et al.*, "Polarization and centre-of-mass energy calibration at FCC-ee", doi:10.48550/arXiv.1909.12245

[5] Y. Wu *et al.*, "Spin polarization simulations for the Future Circular Collider e+e- using Bmad", in *Proc. eeFACT'22*, Frascati, Italy, Sep. 2022, TUZAS0104, pp. 103–107, 2023.

[6] E. Gianfelice-Wendt, "Investigation of beam self-polarization in the future e+ e- circular collider", *Phys. Rev. Accel. Beams*, vol. 19, p. 101005, 2016.
doi:10.1103/PhysRevAccelBeams.19.101005

[7] Y. Wu, "Simulations of the Spin Polarization for the Future Circular Collider e+e- using Bmad", Master's thesis, EPFL, 2022.

[8] D. Sagan, "Bmad, a subroutine library for relativistic charged-particle dynamics", Accessed 24/04/2023,
https://www.classe.cornell.edu/bmad

[9] D. P. Barber *et al.*, "High spin polarization at the HERA electron storage ring", *Nucl. Instrum. Meth. Phys. Res. Sect. A*, vol. 338, pp. 166–184, 1994.
doi:10.1016/0168-9002(94)91311-0

[10] D. P. Barber *et al.*, "A general harmonic spin matching formalism for the suppression of depolarisation caused by closed orbit distortion in electron storage rings", No. DESY-85-044, DESY, 1985.

[11] R. Rossmanith and R. Schmidt, "Compensation of depolarizing effects in electron-positron storage rings", *Nucl. Instrum. Meth. Phys. Res. Sect. A*, vol. 236, pp. 231–248, 1985.
doi:10.1016/0168-9002(85)90156-1

[12] R. Schmidt, "Polarisationsuntersuchungen am Speicherring PETRA", No. DESY-M-82-22, DESY, 1982.

[13] L. H. Thomas, "The kinematics of an electron with an axis", *The London, Edinburgh, and Dublin Philosophical Magazine and Journal of Science*, vol. 3, pp. 1–22, 1927.

[14] V. Bargmann, L. Michel, and V. L. Telegdi, "Precession of the polarization of particles moving in a homogeneous electromagnetic field, in *Phys. Rev. Lett.*, vol. 2, p. 435, 1959.
doi:10.1103/PhysRevLett.2.435

[15] K. Heinemann and G. H. Hoffstätter, "Tracking algorithm for the stable spin polarization field in storage rings using stroboscopic averaging", *Phys. Rev. E*, vol. 54, p. 4240, 1996.

[16] D. P. Barber, G. Ripken, Sections 2.6.6a-2.6.8, in *Handbook of Accelerator Physics and Engineering*, A. W. Chao, M. Tigner, H. Weise, F.Zimmermann (Eds.), 3rd Edn., World Scientific, Singapore, 2023.

[17] A. A. Sokolov and M. Ternov, "On polarization and spin effects in the theory of synchrotron radiation", *Sov. Phys.-Dokl.*, vol. 8, pp. 1203–1205, 1964.

[18] Y. S. Derbenev and A. M. Kondratenko, "Polarization kinetics of particles in storage rings", *Sov. Phys. JETP*, vol. 37, pp. 968–973, 1973.

[19] S. R. Mane, "Derivation of the equilibrium degree of polarization in high-energy electron storage rings", in *Phys. Rev. Lett*, vol. 57, p. 78, 1986. doi:10.1103/PhysRevLett.57.78

[20] D. P. Barber, J. A. Ellison, and K. Heinemann, "Quasiperiodic spin-orbit motion and spin tunes in storage rings", *Phys. Rev. Spec. Top. Accel Beams*, vol. 7, p. 124002, 2004.
doi:10.1103/PhysRevSTAB.7.124002

[21] "FCC-ee optics repository", Accessed 24/04/2023,
https://gitlab.cern.ch/acc-models/fcc/fcc-ee-lattice/-/tree/V18/lattices/z

[22] D. Sagan, "The Tao Manual", Accessed 24/04/2023,
https://www.classe.cornell.edu/bmad/tao.html

[23] D. Sagan, "Long Term Tracking Program", Accessed 24/04/2023, https://www.classe.cornell.edu/bmad/other_manuals.html

[24] "FCC-ee optics repository", Accessed 24/04/2023,
https://gitlab.cern.ch/acc-models/fcc/fcc-ee-lattice/-/tree/V22\?ref_type=heads